IEEE Access
Multidisciplinary | Rapid Review | Open Access Journal

Received April 7, 2019, accepted April 28, 2019, date of publication May 7, 2019, date of current version May 29, 2019.

Digital Object Identifier 10.1109/ACCESS.2019.2915284

Transmission Capacity Analysis for Underlay Relay-Assisted Energy Harvesting Cognitive Sensor Networks

HONG JIANG, HAO YANG, YING LUO, QIUYUN ZHANG, AND MIN ZENG

College of Information Engineering, Network and Communication Research Institute, Southwest University of Science and Technology, Mianyang 621010, China

Corresponding author: Hong Jiang (jianghong@swust.edu.cn)

This work was supported by the National Natural Science Foundation of China under Grant 61771410.

ABSTRACT Energy harvesting cognitive radio sensor networks (EH-CRSNs) are an emerging technology for low-cost, green monitoring of a wide range of environments. How to analyze the transmission capacity is a fundamental and challenging problem in EH-CRSNs due to the dynamics of spectrum and energy arrivals. In this paper, transmission capacity analysis of underlay relay-assisted EH-CRSNs is considered, where some nodes serve as decode-and-forward relays to assist the communication between one secondary source and one destination node. To characterize the end-to-end performance of underlay relay-assisted EH-CRSNs, we first assume that EH devices use harvest–store–use (HSU) mode and formulate the battery states with M/M/1/c model for the arbitrary integer value of transmission energy level threshold. Then, the closed-form expressions of transmission capacity are derived for the random, the nearest, and the farthest relay selection, respectively, based on stochastic geometry. In addition, the transmission capacities with the variable source–destination distance are also analyzed for the three kinds of relay selections. Finally, numerical simulations show that the transmission capacity of underlay relay-assisted EH-CRSNs can be influenced by large amounts of factors, including secondary access probability, source–destination distance, signal-to-interference ratio, and battery transmission energy level threshold, and the different relay selection schemes. The results also confirm that the random relay selection, compared with the nearest and farthest relay selection, is a more feasible and reasonable scheme for short range of underlay EH-CRSNs due to its low complexity implementation.

INDEX TERMS Energy harvesting, cognitive radio sensor networks, relay selection, transmission capacity, access probability.

I. INTRODUCTION

The continuous development of wireless sensor networks (WSNs) will lead to the substantial deployment of sensor nodes and a large exchange of information, aggravating the shortage of spectrum resource and energy of nodes powered by limited battery capacity. Energy harvesting cognitive radio sensor networks (EH-CRSNs) are promising technology solutions for the highly dense and long term networks with considerable impacts on wide monitoring applications, which have recently attracted an increasing research attention [1]–[3]. Furthermore, EH-CRSNs can enhance spectrum efficiency by CR, extend the network lifetime by energy harvesting and improve network performance by relay-assisted transmission [4], [5]. However, the transmission capacity of EH-CRSNs still remains broadly unknown, which is addressed in this paper.

Compared to overlay model powered by EH [6], underlay is more suitable for EH scenarios since sensing operation will lead to high energy consumption. So our main focus is on considering an underlay relay-assisted EH-CRSN powered by rechargeable batteries where all secondary nodes are equipped with a single antenna and operate in a half-duplex mode. Also, we assume that there is no direct link between source and destination, and the communication can be forwarded by one of the relays within a radian sector relaying region Γ with a central angle θ by decode and forward (DF) protocol. Specifically, this paper analyzes the transmission capacity of underlay relay-assisted EH-CRSNs for three relay selection schemes: i) random relay selection,

The associate editor coordinating the review of this manuscript and approving it for publication was Khaled Rabie.

ii) relay selection based on the nearest distance, and iii) relay selection based on the farthest distance. Examples of such settings are applicable to practical cases when we need to deploy short range surveillance WSNs powered by rechargeable batteries which are impossible for frequent replacement [7].

Although the harvested energy is limited in dynamic energy arrival environments, it may be enough for low-power EH-CRSNs to support the data transmission in underlay model. Specifically, secondary nodes can access licensed spectrum at any time subject to the interference power constraint and the energy causality constraint. In general, energy harvested in wireless networks can be dealt in the following two modes [8]. The first is the Harvest-use (HU) mode where a node has no battery and the harvested energy cannot be stored. The second is the Harvest-store-use (HSU) mode where a node has battery and the stored energy beyond a threshold can be used to transmit data [9], which is generally used in dynamic harvesting environments. In this paper, we assume that both secondary source and relay nodes apply HSU mode.

For HSU mode in EH-WNSs, it is usually assumed that either source or relay node can perform EH. This assumption is generally accepted in the literature, mainly because it facilitates the analysis by avoiding simultaneously modeling for both source and relay batteries [9]–[11]. In [9] Lee *et al.* considered a low-power requirement with RF energy harvesting in EH-CRN, where a secondary transmitter (ST) harvests ambient energy from active primary transmitters (PTs) and stores the energy in a battery with finite capacity equal to the minimum energy required for one-slot transmission. Besides, in [10], Chen *et al.* assumed that PT and ST collect and store ambient energy, and analyzed the transmission and coverage probabilities for both PT and ST with infinite battery. In [11], the performance of cache-assisted simultaneous wireless information and power transfer cooperative systems was studied, in which one source communicate with one destination via the aid of multiple relays with energy harvesting capability. In [12], the performance of large-scale cooperative wireless networks powered by EH was characterized based on stochastic geometry, in which only transmitter can harvest and store the energy. Furthermore, in [13] Jeon and Ephremides explored the impact of random access with EH on stability in which node stored the harvested energy in finite-capacity battery and the state of battery was formulated as M/M/1/c queueing model. It is worth noting that the Markov chain model of battery state adds an additional assumption that a node can transmit when its battery energy level exceeds a threshold value of one [9], [12], [14], which may be unsuitable for practical applications. Consequently, the performance of EH-CRSN needs to be reanalyzed to account for the new challenges such as arbitrary transmission energy level thresholds and dynamic energy availabilities when both source and relay nodes are powered by EH.

Relay-assisted transmission is an important technology to enhance the capacity and coverage of CRNs when there do not exist direct paths between source and destination node [4], [15]–[17]. In [4], the outage probability and the ergodic capacity of the underlay secondary decode-and-forward (DF) system with the Nth best relay selection were analyzed. Similarly, in [15], the outage probability and ergodic capacity bounds of multiuser multiple antenna amplify-and-forward relaying networks with opportunistic scheduling were studied. Furthermore, in [16] and [17], outage performance was studied for the case of dual-hop in underlay CRNs. In addition, the performance of spatial throughput for positive forward progress with multi-hop relay was analyzed in cognitive underlay networks in [18].

The combination of relaying and EH is very fundamental to enhance the capacity and prolong the network lifetime in EH-CRNs[19]–[22]. After adding ability of EH, an EH protocol and outage probability were investigated for an underlay cognitive relay network in [19], where secondary users harvest energy from primary network. Similarly, the outage probability and the optimal relay location of wireless EH relay-assisted underlay CR with HU model was analyzed in [20]. Also, a dual-hop relay system in which the source transmitter and the relay are both equipped with fixed EH battery was considered in [21], where the ergodic capacity with respected to the end-to-end signal-to-noise ratio (SNR) was derived. In addition, the effects of relay selection in wireless powered networks equipped with batteries on outage probability were investigated in [22]. Unfortunately, in relay-assisted EH-CRSNs with hard resource constraints, an unavoidable fact is that nodes can only perform simple relay selection algorithms, such as the random relay selection, the nearest relay selection, or the farthest relay selection. As a result, the effects of these different relay selection algorithms on transmission performance of relay-assisted EH-CRSNs need to be analyzed.

As one of the key performance metrics of the wireless system, the transmission capacity analysis faces to a critical challenge due to the dynamic influences from spectrum or energy arrivals [4], [14], [23]–[25]. The ergodic capacity of the secondary system with a single relay was derived in [4]. In [14], the transmission capacity of wireless ad-hoc networks was investigated, where a node with energy harvesting capacity can transmit when its energy level was greater than a threshold value. Further, Noh *et al.* [23] analyzed the ergodic capacity of the secondary user under an average received-power constraint. In addition, the transmission capacity of relay-assisted D2D communication was analyzed in [24], where D2D users can transmit in overlay or underlay mode. In [25], the end-to-end throughput maximization for underlay multi-hop EH-CRNs was studied, where battery-free SUs capture the energy of PUs to realize the multi-hop communication. However, most existing works seldom explicitly consider the characteristics of the EH-CRSNs when charging both source and relay batteries by energy harvesting.

In this paper, different from [9], [11], [12], [14], we consider a more general case of underlay relay-assisted

EH-CRSNs where secondary source (in the rest of this paper, we use the terms secondary source and secondary transmitter interchangeably) and relay are both equipped with respective battery of finite capacity, and each can transmit data only when its stored energy level in battery exceeds a given threshold value, which may be equal or greater than one. Moreover, also unlike [21], where the main objective is to investigate the performance of the wireless relaying system with respect to SNR under the assumption that the source and the relay are both equipped with fixed EH battery, the objective of this paper is to analyze the transmission capacity of EH-CRSNs by comprehensively considering the effects of key parameters, such as transmission energy level threshold, access probability, source-destination distance and relay selection schemes, etc., based on stochastic geometry [26].

In this study, we analyze the transmission capacity of underlay relay-assisted EH-CRSNs, and the key contributions of this paper are summarized as follows.

- We investigate the transmission capacity of a dual-hop underlay relay-assisted EH-CRSN with respect to comprehensive parameters where both source and relay nodes are powered by HSU model, unlike previous work (e.g. 21]), where the HU approach was considered with respect to SNR.
- In contrast to [12], [14], where the energy arrivals are modeled by a birth-death Markov process M/M/1 with transmission threshold one, we formulate the battery state with M/M/1/c model for an arbitrary integer threshold value of transmission energy level. Also different from [22] where the battery is either full or empty, our reduced two battery states by Markov Chain Cluster are either enough or not enough to transmit, which is more reasonable in practical resource constraint systems.
- Note that different from [22], where only relays are equipped with batteries, and outage probability is derived for different relay selection schemes with respect to SNR, we focus on closed-form expressions for the transmission capacity, under the random relay selection, the nearest relay selection and the farthest relay selection, by jointly considering comprehensive effects of key parameters including transmission energy level and SIR threshold, access probability, battery capacity, and source-destination distance. To the best of the authors' knowledge, the capacity analysis of underlay relay-assisted EH-CRSNs with batteries equipped at both the source and relay, under different relay selection algorithms, has not been reported in the literature.

The remainder of this paper is organized as follows. Section II describes network and energy harvesting model. Section III presents the successful transmission probability and derives the transmission capacity under three kinds of relay selection schemes. Simulation results and discussions are shown in Section IV, where the impacts of various system parameters on transmission capacity are discussed. Finally, the conclusions are summarized in Section V.

II. SYSTEM MODEL

In this section, we outline the network model, channel model, EH model and transmission model. The key parameters used in this paper are given in Table 1.

TABLE 1. Key parameters notations used in this paper.

Symbol	Notation
λ_1, λ_s	The density of PTs and secondary nodes
P_{a1}, P_{a2}, P_{a3l}	The access probability of PT, ST and relay (l=r, n ,f, denote the random, the nearest and the farthest relay)
P_r	The relay existence probability within relaying region
P_g	The probability that there is no ST (or secondary source) or relay within PR guard zone
r_p	Guard zone radius for primary receiver (PR)
ρ_1	The primary transmission power
D	The distance between ST and its intended destination
X_l	The distance variable between ST and relay under the random, the nearest and the farthest relay (l=r, n or f).
S_r, θ	The area and central angle of sector relaying region
α	The path loss exponent
L	The size of discretized energy levels of battery capacity
λ_i	The density of STs or potential relays, $i \in \{2, 3\}$
ρ_i	Transmission power level threshold of i node
γ_i	SIR threshold of i node,
$P_i^{j,k}$	The battery transition probability from state j to k of i node
π_i^j	The steady probability of the i node battery is in state j
μ_i	The energy arrivals rate of i node
$\eta_2^{sl}(P_{a2}, \mu_2)$	The steady state probability of ST's energy level larger than transmission power level threshold
$\eta_3^{sl}(P_{a3l}, \mu_3)$	The steady state probability of relay's energy level larger than transmission power level threshold (l=r, n or f)

A. NETWORK MODEL

As shown in Fig.1 (a), we consider a dual-hop EH-CRSN working in time division duplex (TDD) model. The primary network transmitters follow a homogeneous Poisson point process (HPPP) Π_1, with density λ_1, and access the spectrum with probability P_{a1} and transmission power ρ_1. In addition, each primary transmitter communicates with its intended receiver which is associated with a guard zone with radius r_p to avoid interference from the secondary sources or transmission relays [9]. Thus, only secondary sources or potential relays outside the primary's guard zone can be active and the probability that there is no primary receiver (PR) inside the disk centered at secondary sources or relays is given by $P_g = \exp(-\pi P_{a1}\lambda_1 {r_p}^2)$. Likewise, let secondary nodes, including sources and potential relays, follow HPPP with density λ_s and a source access the licensed spectrum with probability P_{a2} under transmission power level ρ_2. Via a certain relay selection scheme, one of the potential relays within a radian sector region with a central angle θ is selected to forward the information from the source to the destination by DF protocol. According to the Coloring Theorem, the secondary sources O_s form a HPPP Π_2 with density $\lambda_2 = \lambda_s P_{a2}$ and the receivers (potential relays) follow another HPPP Π_3 with density $\lambda_3 = \lambda_s(1 - P_{a2})$. Additionally, let each secondary source O_s have an intended destination D_s at a distance D.

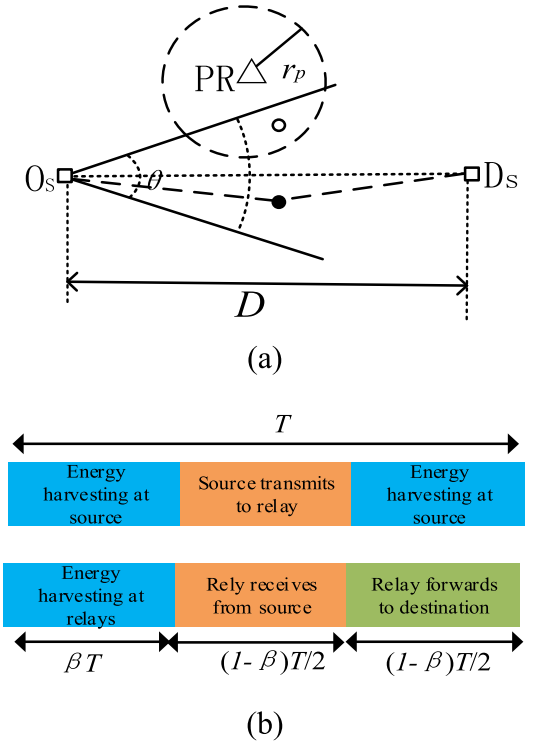

FIGURE 1. System model. (a) Secondary source-destination underlay communication assisted by relays, where a triangle denotes a primary receiver, two squares are secondary source and destination respectively, and a solid circle denotes a transmission relay which can forward source data to destination, while a hollow circle is a potential relay which cannot forward data since it lies in the guard zone of the PR.
(b) Harvest-store-transmit protocol.

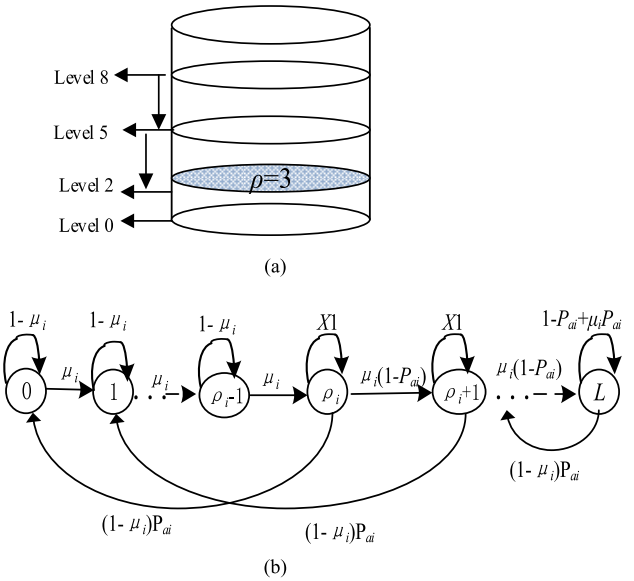

FIGURE 2. The battery power state transition and the corresponding $L+1$-state Markov chain model, where (a) denotes an example of battery state transition with two transmission events from level 8 to level 2; an example of battery power state of the source or relay with $\rho = 3$.
(b) Finite state Markov chain for finite battery buffer with $X1 = (1-\mu_i)(1-P_{ai}) + \mu_i P_{ai}$.

We assume that all three types of channels, i.e., primary-to-secondary; secondary-to-secondary and secondary-to-secondary, suffer from both small-scale block fading and large-scale path-loss effects. Specifically, the channel gain is modeled by $Hd^{-\alpha}$, where H is a unit mean exponentially distributed random variable which accounts for the small scale Rayleigh fading channel, d is the distance between the transmitter and the receiver and $\alpha \geq 2$ is the path loss exponent. In addition, it is assumed that the communication is interference limited and hence thermal noise is negligible.

B. ENERGY HARVESTING MODEL

Both secondary source and relay are equipped with energy harvesting modules and batteries with finite capacities B. Let the size of battery be discretized in $L+1$ energy levels kB/L with $k = 0, 1, \ldots, L$ [27]. We assume that the energy packet arrivals at the source and relay battery with rate μ_i ($i \in \{2, 3\}$, where 2 stands for source node, and 3 denotes relay node) are assumed to be independent and identically distributed (IID) Bernoulli process [12]. As shown in Fig.1 (b), the source harvests energy for a duration of $(1+\beta)T/2$, while the relays harvest energy for a duration of βT, where T is the duration of one time slot and $0 < \beta < 1$. Subsequent to the harvesting period, the selected relay first receives information from the source for a duration of $(1-\beta)T/2$, and then forwards the information to the destination for an another duration of $(1-\beta)T/2$. To simplify the analysis, we let $\beta = 1/3$ as in reference [20]. Both source and relay access with probability P_{ai} (service rate) and transmit with fixed power level ρ_i ($< L$), which means that when the power level of a battery is greater than or equal to a threshold value ρ_i, the transmission will lead to a state transform from j ($\geq \rho_i$) to j-ρ_i. Fig.2 (a) presents an example of this model, in which we assume the transmission power level threshold $\rho = 3$ and the battery current level is 8. So there are at most two transmission events: the first transmission will lead to the battery state being reduced from level 8 to 5; and the second transmission will make a transition from level 5 to 2. When the battery level becomes 2, the node cannot transmit until it harvests enough energy (e.g. energy level becomes more than ρ). Thus, similar to [12], [13], we assume that the power level of battery $B_i(t)$ follow a decoupled discrete time $M/M/1/c$ queueing model, with input rate μ_i, service rate P_{ai} and capacity $L+1$ as shown in Fig. 2 (b) [28].

The probability that the battery is in j is given by:

$$\pi_i^j = \begin{cases} \pi_i^{j-1} P_i^{j-1,j} + \pi_i^j P_i^{j,j} + \pi_i^{j+\rho_i} P_i^{j+\rho_i,j}, & 0 \leq j \leq L-\rho_i \\ \pi_i^{j-1} P_i^{j-1,j} + \pi_i^j P_i^{j,j}, & L-\rho_i < j \leq L \end{cases} \tag{1}$$

where π_i^j denotes the steady probability that the ith ($i \in \{2, 3\}$) type of node is at state j (note that $\pi_i^{-1} = 0$ denotes a nonexistent virtual sate for ease of presentation) and $P_i^{j,k}$ denotes the transition probability from state j to k of ith node battery. Furthermore, we can derive from Fig.2 (b) that when $j < \rho_i$, $P_i^{j-1,j} = \mu_i$, $P_i^{j,j} = 1-\mu_i$; $j = \rho_i$, $P_i^{j-1,j} = \mu_i$,

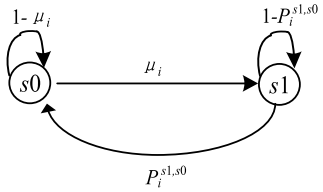

FIGURE 3. Reduced state of battery.

$P_i^{j,j} = X1$; $\rho_i < j < L$, $P_i^{j-1,j} = \mu_i(1 - P_{ai})$, $P_i^{j,j} = X1$; $j = L$, $P_i^{j-1,j} = \mu_i(1-P_{ai})$, $P_i^{j,j} = 1-P_{ai}+\mu_i P_{ai}$. In addition, when $0 \le j \le L$-ρ_i, $P_i^{j+\rho_i,j} = (1 - \mu_i)P_{ai}$.

Let $\mathbb{Z}^i = (P_i^{j,k})$ denote $(L + 1) \times (L + 1)$ battery state transition matrix of the Markov Chain (MC) for the ith type of node. Since the matrix is irreducible and row stochastic, there must exist a unique stationary distribution $\pi_i = (\pi_i^0, \pi_i^1, \ldots, \pi_i^L)^T$, which can be obtained by solving equilibrium equation under the constraint $\sum_{j=0}^{L} \pi_i^j = 1$. Obviously, when L is large, the solving overhead may be prohibitively expensive for EH-CRSN. To ease the computation, we reduce $L + 1$ states to only two states (e.g. $s0$ and $s1$ as shown in Fig.3) by MC Cluster[28]. More specifically, the battery is in $s0$ if its energy level is less than ρ_i and in $s1$ otherwise. In other words, the probability that the battery is at state s0 in Fig. 3 (e.g. the battery energy is insufficient to transmit information) equals to the summation of probabilities of all states less than ρ_i in Fig.2 (b), and the probability that the battery stays in state s1 in Fig..3 (e.g. the battery energy is sufficient to transmit information) is the summation of probabilities of all states larger than $\rho_i - 1$ in Fig.2 (b). Note that this two battery states seems to be similar to [22] where the battery level is represented by empty and charged. But our two battery states are significantly different since we focus on a more general battery level model with sufficient or insufficient energy to transmit.

The transition probability from s_1 to s_0 is given by:

$$P_i^{s1,s0} = \begin{cases} (1 - \mu_i)P_{ai}(\dfrac{\pi_i^{\rho_i} + \pi_i^{\rho_i+1} + \ldots + \pi_i^{2\rho_i-1}}{\pi_i^{\rho_i} + \pi_i^{\rho_i+1} + \ldots + \pi_i^{L}}) \\ \qquad 2\rho_i - 1 < L \\ (1 - \mu_i)P_{ai} \quad \rho_i \le L \le 2\rho_i - 1 \end{cases} \tag{2}$$

For simplicity of illustration, let $A_\pi = \pi_i^{\rho_i} + \pi_i^{\rho_i+1} + \ldots + \pi_i^{2\rho_i-1}$, $B_\pi = \pi_i^{\rho_i} + \pi_i^{\rho_i+1} + \ldots + \pi_i^{L}$. From (1) and (2), the probability of steady state $s0$ and $s1$ can be derived as

$$\eta_i^{s0}(P_{ai}, \mu_i) = \begin{cases} (\dfrac{(1 - \mu_i)P_{ai}A_\pi}{(1 - \mu_i)P_{ai}A_\pi + \mu_i B_\pi}) & 2\rho_i - 1 < L \\ \dfrac{(1 - \mu_i)P_{ai}}{(1 - \mu_i)P_{ai} + \mu_i} & \rho_i < L \le 2\rho_i - 1 \end{cases} \tag{3}$$

$$\eta_i^{s1}(P_{ai}, \mu_i) = \begin{cases} (\dfrac{\mu_i B_\pi}{(1 - \mu_i)P_{ai}A_\pi + \mu_i B_\pi}) & 2\rho_i - 1 < L \\ \dfrac{\mu_i}{(1 - \mu_i)P_{ai} + \mu_i} & \rho_i < L \le 2\rho_i - 1 \end{cases} \tag{4}$$

From (3) or (4), it is obvious that the two battery states steady probability of node i is a function of both $P_{\rm ai}$ and $\mu_{\rm i}$.

III. TRANSMISSION CAPACITY ANALYSIS

In this section, the transmission capacity of underlay relay-assisted EH-CRSNs is analyzed.

The probability $P_{\rm r}$ that there is at least one potential relay inside the relaying region is given by

$$P_r = 1 - e^{-S_r\lambda_3} \tag{5}$$

where $S_r = \frac{\theta}{2}D^2$ denotes the area of relaying region.

Since the relay transmission is performed in a TDD way, the density of activated source or relay is denoted as $\lambda_{al} = \frac{1}{2}\lambda_2 \cdot P_g \cdot \eta_2^{s1}(P_{a2}, \mu_2) \cdot P_r \cdot P_g \cdot \eta_3^{s1}(P_{a3l}, \mu_3)$, where $l \in \{r, n, f\}$, denotes the random, the nearest and the farthest relay selection scheme, respectively.

A. RANDOM RELAY SELECTION ROUTING (RRS)

In RRS routing, a secondary source will randomly choose a relay to help transmission, which means a low complexity implementation suitable for sensor networks with strict power/bandwidth constraints. The arc length $l(x)$ with secondary source as center and x as radius across the relaying region is $l(x) = \theta x$, and the probability density function of x is $f_{X_r}(x) = \frac{2x}{D^2}$. Thus, the expectation of distance between secondary source and relay is given by

$$E(X_r) = \frac{2}{D^2}\int_0^D x^2 dx = \frac{2}{3}D \tag{6}$$

The average access probability of the selected relay for random selection is given by

$$\mathrm{P}_{a3r} = P_{a2}\frac{E[X_r]}{D} = 2P_{a2}/3 \tag{7}$$

Then the density of activated source or relay is obtained as

$$\lambda_{ar} = \frac{1}{2}\lambda_2 \cdot P_g \cdot \eta_2^{s1}(P_{a2}, \mu_2) \cdot P_r \cdot P_g \cdot \eta_3^{s1}(P_{a3r}, \mu_3) \tag{8}$$

where η^{s1}, P_r and $P_{\rm a3r}$ can be obtained by (4), (5) and (7), respectively. It is noted that the rationale behind (8) is that both secondary source and potential relay with enough energy and locating outside the guard zone can communicate with each other.

B. RELAY SELECTION WITH THE NEAREST DISTANCE FROM ST (RSN)

It is assumed that a secondary source obtains a priori information of the potential relays' locations through a low rate feedback channel or a Global Positioning System (GPS) mechanism, and selects the nearest nodes to forward signals.

Proposition 1: Let $X_{\rm n}$ denote the distance between the ST and the nearest node, and the density of source or relay without considering relay battery status is denoted as $\lambda_{an1} = \frac{1}{2}\lambda_2 P_g \eta_2^{s1}(P_{a2,}\mu_2)P_r P_g$. The mean distance is derived as follows

$$E(X_n) = \frac{C_1 - D\exp(-\frac{\theta\lambda_{an1}}{2}D^2)}{1 - \exp(-\frac{\theta\lambda_{an1}}{2}D^2)} \tag{9}$$

with

$$C_1 = \sqrt{\frac{\pi}{2\theta\lambda_{ar1}}} erf(\frac{D}{2}\sqrt{2\theta\lambda_{ar1}})$$

where erf(.) is the error function as follows

$$erf(x) = \frac{2}{\sqrt{\pi}} \int_0^x e^{-t^2} dt$$

Proof: See Appendix A

Using the expression (9), the average access probability of a relay for the nearest selection is given by

$$P_{a3n} = P_{a2} \frac{E[X_n]}{D} \tag{10}$$

Then the density of activated transmitter or relay is denoted as

$$\lambda_{an} = \frac{1}{2}\lambda_2 \cdot P_g \cdot \eta_2^{s1}(P_{a2}, \mu_2) \cdot P_r \cdot P_g \cdot \eta_3^{s1}(P_{a3n}, \mu_3) \tag{11}$$

C. RELAY SELECTION WITH THE FARTHEST DISTANCE FROM ST (RSF)

Assuming that the locations of potential relays in relaying region are known at STs, which can be realized by similar methods as in RSN. Then, the ST will select the farthest node to forward signals. Let X_f denote the distance between the secondary source and the farthest node, and the density of source or relay without considering relay battery status is denoted as $\lambda_{af1} = \frac{1}{2}\lambda_2 \cdot P_g \cdot \eta_2^{s1}(P_{a2}, \mu_2) \cdot P_r \cdot P_g$. Then, the mean distance is derived as follows

$$E(X_f) = \frac{D\exp(\frac{\theta\lambda_{af1}}{2}D^2) - C_2}{\exp(\frac{\theta\lambda_{af1}}{2}D^2) - 1} \tag{12}$$

with

$$C_2 = \sqrt{\frac{\pi}{2\theta\lambda_{af1}}} erfi(\frac{D}{2}\sqrt{2\theta\lambda_{af1}})$$

where erfi(.) is the imaginary error function as follows

$$erfi(x) = \frac{2}{\sqrt{\pi}} \int_0^x e^{t^2} dt$$

Proof: See Appendix B

According to result of (12), the access probability of a relay for the farthest selection is given by

$$P_{a3f} = P_{a2} \frac{E[X_f]}{D} \tag{13}$$

Then the density of activated source or relay for the farthest node is denoted as

$$\lambda_{af} = \frac{1}{2}\lambda_2 \cdot P_g \cdot \eta_2^{s1}(P_{a2}, \mu_2) \cdot P_r \cdot P_g \cdot \eta_3^{s1}(P_{a3f}, \mu_3) \tag{14}$$

D. TRANSMISSION CAPACITY ANALYSIS

In order to obtain the successful transmission probability of a typical receiver, all three types of interferences from primary users, secondary source users, and relays are considered. Reliable transmission means that the SIR of the receiver in Π_i should meet $\mathrm{SIR}_i > \gamma_i$, where γ_i is the SIR threshold of $\Pi_i (i \in \{2, 3\})$. Thus, the general form of successful transmission probability of a typical receiver in Π_i is given by (15), as shown at the bottom of this page.

Where $K_\alpha = 2\pi^2/(\alpha \sin(2\pi/\alpha))$, r_i is the distance from the desired transmitter to the typical receiver, and $L_{I_1}(s)$, $L_{I_2}(s)$, and $L_{I_3}(s)$ are Laplace transformation of I_1, I_2 and I_3, respectively.

After obtaining the successful transmission probability, the transmission capacity can be computed by the product of user density and the successful transmission probability [26]. For convenience, let both source and relay transmit with the same power level and receive with the same SIR threshold, respectively, i.e. $\gamma_2 = \gamma_3$, $\rho_2 = \rho_3$. In addition, for ease of presentation, let

$$w_{2l} = K_a \cdot \gamma_2^2 \cdot [\lambda_1 \cdot (\frac{\rho_1}{\rho_2})^{2/\alpha} + \lambda_{al} + \lambda_{al} \cdot (\frac{\rho_3}{\rho_2})^{2/\alpha}],$$
$$w_{3l} = K_a \cdot \gamma_2^2 \cdot [\lambda_1 \cdot (\frac{\rho_1}{\rho_3})^{2/\alpha} + \lambda_{al} \cdot (\frac{\rho_2}{\rho_3})^{2/\alpha} + \lambda_{al}],$$

where $l \in \{r, n, f\}$, denotes the random, the nearest and the farthest relay selection scheme, respectively. Since $\gamma_2 = \gamma_3$, $\rho_2 = \rho_3$, then $w_{2l} = w_{3l}$.

$$\Pr(SIR_{sr} > \gamma_2) = \exp(-w_{2l} \cdot r_2^2)$$
$$\Pr(SIR_{rd} > \gamma_2) = \exp(-w_{3l} \cdot r_3^2)$$

1) TRANSMISSION CAPACITY WITH RRS

According to (6), (7) and (8), the source-relay-destination transmission capacity under random relay selection is given by

$$\begin{aligned} C_{sd-r} &= \lambda_{ar} \cdot \Pr(SIR_{sr} > \gamma_2) \times \Pr(SIR_{rd} > \gamma_2) \\ &= \lambda_{ar} \cdot \exp[-2w_{2r} \cdot E^2(X_r)] \end{aligned} \tag{16}$$

$$\begin{aligned} \Pr\{SIR_i \geq \gamma_i\} &= \Pr\{\frac{\rho_i H_i r_i^{-\alpha}}{\sum_{j\in\prod_1} \rho_1 H_j |x_j|^{-\alpha} + \sum_{k\in\prod_2} \rho_2 H_k |y_k|^{-\alpha} + \sum_{m\in\prod_2} \rho_3 H_m |z_m|^{-\alpha}} \geq \gamma_i\} \\ &= \Pr\{H_i \geq \frac{\gamma_i r_i^\alpha}{\rho_i}[\sum_{j\in\prod_1} \rho_1 H_j |x_j|^{-\alpha} + \sum_{k\in\prod_2} \rho_2 H_k |y_k|^{-\alpha} + \sum_{m\in\prod_3} \rho_3 H_m |z_m|^{-\alpha}]\} \\ &= L_{I_1}(\frac{\gamma_i x^\alpha}{\rho_i}) L_{I_2}(\frac{\gamma_i x^\alpha}{\rho_i}) L_{I_3}(\frac{\gamma_i x^\alpha}{\rho_i}) \\ &= \exp(-K_\alpha \cdot \gamma_i^{\frac{2}{\alpha}} \cdot r_i^2 [\lambda_1 (\frac{\rho_1}{\rho_i})^{\frac{2}{\alpha}} + \lambda_2 (\frac{\rho_2}{\rho_i})^{\frac{2}{\alpha}} + \lambda_3 (\frac{\rho_3}{\rho_i})^{\frac{2}{\alpha}}]) \end{aligned} \tag{15}$$

2) TRANSMISSION CAPACITY WITH RSN

From (9), (10) and (11), the source-relay-destination transmission capacity under the nearest relay selection is given by

$$\begin{aligned} C_{sd-n} &= \lambda_{an} \cdot \Pr(SIR_{sr} > \gamma_2) \times \Pr(SIR_{rd} > \gamma_2) \\ &= \lambda_{an} \cdot \exp[-2w_{2n}E^2(X_n)] \end{aligned} \tag{17}$$

3) TRANSMISSION CAPACITY WITH RSF

From (12), (13) and (14), the source-relay-destination transmission capacity under the farthest relay selection is given by

$$\begin{aligned} C_{sd-f} &= \lambda_{af} \cdot \Pr(SIR_{sr} > \gamma_2) \times \Pr(SIR_{rd} > \gamma_2) \\ &= \lambda_{af} \cdot \exp[-2w_{2f}E^2(X_f)] \end{aligned} \tag{18}$$

E. TRANSMISSION CAPACITY WITH VARIABLE S-D DISTANCE

In above analysis, the source-destination distance D is a given value. In practical deployment of networks, however, the distance D usually is a random variable. For convenience, we assume the distance D follows uniform distribution in $[D_1, D_2]$ with PDF $f_D(d) = \frac{1}{D_2 - D_1}$, where $d \in [D_1, D_2]$.

1) TRANSMISSION CAPACITY WITH RANDOM SELECTION

For ease of illustration, let

$$\begin{aligned} C_3 &= erf(2\sqrt{w_{2r}}D_2/3) - erf(2\sqrt{w_{2r}}D_1/3), \\ C_4 &= erf(2\sqrt{w_{3r}}D_2/3) - erf(2\sqrt{w_{3r}}D_1/3) \end{aligned}$$

Then, the transmission capacity for the random relay selection with variable D under uniform distribution is derived as follows:

$$\begin{aligned} &C_{sd-r-ud} \\ &= \frac{\lambda_{ar}}{(D_2 - D_1)^2} \int_{D_1}^{D_2} \exp(-\frac{4w_{2r}}{9}r^2)dr \\ &\quad \cdot \int_{D_{\min 1}}^{D_{\max}} \exp(-\frac{4w_{3r}}{9}r^2)dr \\ &\overset{(a)}{=} \frac{9\lambda_{ar}\pi \cdot C_3 \cdot C_4}{16(D_2 - D_1)^2\sqrt{w_{2r}w_{3r}}} \\ &\overset{(b)}{=} \frac{9\lambda_{ar}\pi[erf(2\sqrt{w_{2r}}D_2/3) - erf(2\sqrt{w_{2r}}D_1/3)]^2}{16(D_2 - D_2)^2 w_{2r}} \end{aligned} \tag{19}$$

where (a) holds according to [29, eq. (2.33.16)] and (b) holds according to the fact that $C_3 = C_4$ due to $w_{2r} = w_{3r}$.

2) TRANSMISSION CAPACITY WITH THE NEAREST SELECTION

From the expression of $\mathrm{E}[X_n]$, it is difficult to derive the exact closed form of capacity for the nearest relay selection with variable S-D distance. However, for $\theta\lambda_{an1} \approx 0$, by using the approximations $\exp(-x) \approx 1 - x$ and $\frac{\sqrt{\pi}}{2}erf(x) \approx x - \frac{1}{3}x^3$ [29, eq. (3.321.1)], we can derive the approximations $C_1 \approx D - \frac{\theta\lambda_{an1}}{6}D^3$ and $E(X_n) \approx \frac{2}{3}D$. Similarly to (19), the transmission capacity for the nearest relay selection with variable D under uniform distribution is derived as follows:

$$C_{sd-n-ud} \approx \frac{9\lambda_{an}\pi[erf(2\sqrt{w_{2n}}D_2/3) - erf(2\sqrt{w_{2n}}D_1/3)]^2}{16(D_2 - D_1)^2 w_{2n}}$$

3) TRANSMISSION CAPACITY WITH THE FARTHEST SELECTION

Similarly, for $\theta\lambda_{af1} \approx 0$, by using the approximations $\exp(x) = 1 + x$ and $erfi(x) \approx erf(x)$, we can again obtain $E(X_f) \approx \frac{2}{3}D$. Then, the transmission capacity for the farthest relay with variable D under uniform distribution is given by:

$$C_{sd-f-ud} \approx \frac{9\lambda_{af}\pi[erf(2\sqrt{w_{2f}}D_2/3) - erf(2\sqrt{w_{2f}}D_1/3)]^2}{16(D_2 - D_1)^2 w_{2f}}$$

IV. SIMULATION RESULTS AND DISCUSSIONS

In this section, we present simulation results on the transmission capacity of underlay relay-assisted EH-CRSN to validate the above theoretical results. Throughout this section, unless otherwise specified, the values for the key simulation parameters of Table 1 are listed in Table 2.

TABLE 2. Main simulation parameters.

Parameters	Default value
The density of PTs λ_1	0.0001
The density of secondary nodes λ_s	0.0008
The access probability of PTs P_{a1}	0.8
The ratio of transmission power of PT and secondary source ρ_1/ρ_2	2.3
The ratio of transmission power of secondary source and relay ρ_2/ρ_3	1
The radius of guard zone of PR r_p	4m
The central angle of sector relaying region θ	$\pi/2$
SIR threshold of secondary source or relay node γ_2, γ_3	2dB
The size of discretized energy levels of battery capacity L	30
The energy arrivals rate of secondary source or relay μ_2 , μ_3	0.51
The path loss exponent α	4
the duration of one time slot	3

Fig. 4 depicts the secondary transmission capacity of underlay relay-assisted EH-CRSNs with varying access probability P_{a2} and distance D for three kinds of relay selection schemes. We can see that the capacity of shorter distance D is always greater and varies more rapidly than the cases with longer distances. The reason is that shorter distance means less attenuation and the variance of access behavior will become the main factor affecting the transmission capacity. An important observation is that there exists a maximum capacity with respect to P_{a2} approximately equal to 0.35. It should be noted that similar result was observed for spatial throughput with varying secondary access probability [18]. The intuitive interpretation is that increasing the secondary access probability can increase the effective number of concurrent transmission resulting in higher transmission capacity. However, the capacity will decrease with continuous increase in the P_{a2}, which results in higher aggregated interference and a smaller number of relays. In addition, we can see that, for a specified distance D, the capacity of the random selection scheme is always situated in a region smaller than

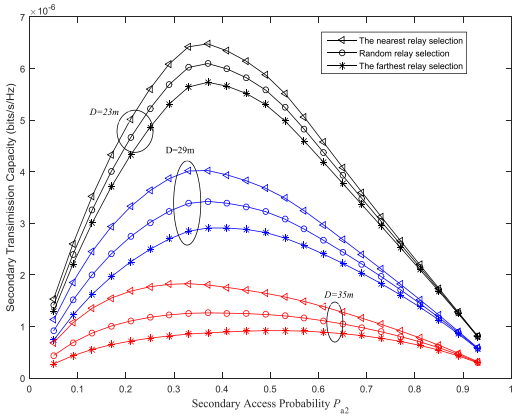

FIGURE 4. Secondary capacity versus P_{a2} for $L = 30$.

the capacity of the nearest selection and greater than one obtained by the farthest selection. Last but not least, another important observation is that the differences of capacities among three relay selection schemes are not significant for short range of wireless communication. Although the nodes' locations can be obtained by GPS, it is not practical to use GPS due to its high power consumption in wireless sensor networks, especially in EH scenarios [30], [31]. In other words, the random relay selection will be a more feasible and reasonable scheme for EH-CRSNs scenarios due to its low complexity implementation. Therefore, we will focus on transmission capacity analysis for the random relay selection in subsequent simulation analyses. It is noted that although the random relay selection is simple, the relay transmission may suffer from longer delay since the selected relay may have insufficient energy, which means that the random relay selection is not suitable for delay-sensitive scenarios.

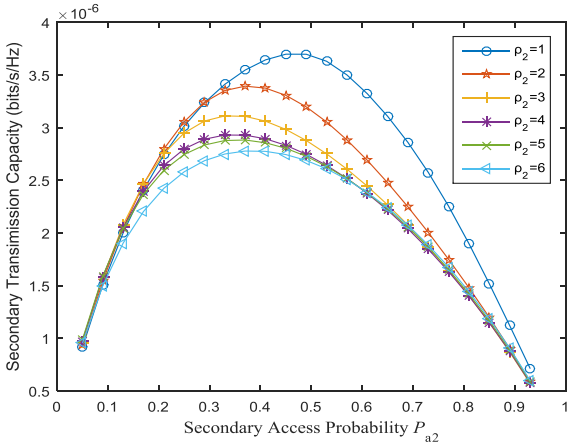

FIGURE 5. Secondary capacity under different ρ_2 for $D = 29$ and $L = 10$.

Shown in Fig.5 is the secondary transmission capacity under different P_{a2} and transmission threshold ρ_2 for random relay selection. As seen in the figure, lower threshold means higher transmission capacity due to the fact that lower threshold will satisfy transmission energy condition more easily. Also, the transmission capacities corresponding to different thresholds remain almost the same for small values of access probability. The reason is that lower access probability can cause higher probability of battery energy level larger than transmission threshold. In addition, we can see from Fig.5 that, when the thresholds are small, the variance of thresholds will cause the more distinctly varying in capacity for P_{a2} in an approximate interval (0.4, 0.8). Moreover, the capacities become approximately same when the transmission thresholds are larger than a specified value, for the example given in Fig.5, $\rho_2 = 4$. Again we observe that maximum capacities for different thresholds will be obtained for P_{a2} values in (0.35, 0.5), similar to the observations from Fig. 4.

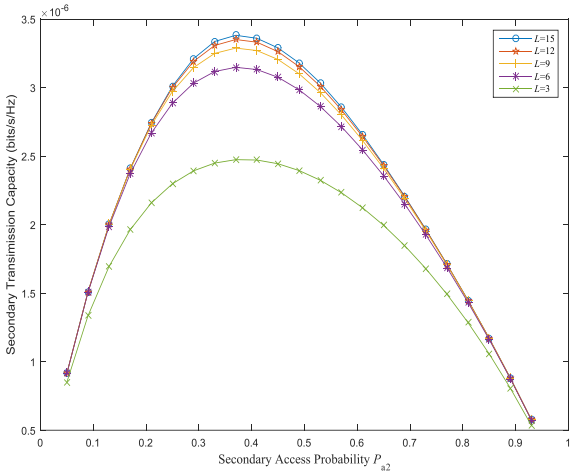

FIGURE 6. Secondary capacity under different battery capacity with $D = 29$ and $\rho_2 = 1$.

Fig.6 illustrates the influence of battery capacity on transmission capacity for random relay selection. As shown, the lower the battery capacity, the smaller the transmission capacity. This is because the stored energy level beyond the transmission threshold is easier to be met when the battery capacity increases. Furthermore, we can see that when the capacities are small, the variances of capacity will lead to apparent change of the transmission capacity. However, when battery capacity exceeds a certain value, see $L \geq 9$, the transmission capacity will tend to be the same for different battery capacities, which doesn't mean the larger battery capacity the better in EH-CRSN scenarios. Similar to Fig. 4 and Fig.5, we observe that the maximum transmission capacities will be obtained when $P_{a2} \approx 0.4$ for different battery capacities.

Fig.7 illustrates the secondary transmission capacity versus SIR threshold and access probability for random relay selection. It is observed that the lower the SIR threshold, the greater the transmission capacity. This can be explained as follows. If SIR threshold is smaller, the relay or destination will be more easily to decode received signals. In addition, the lower SIR threshold also means more dramatic change of capacity with respect to access probability. However, lower

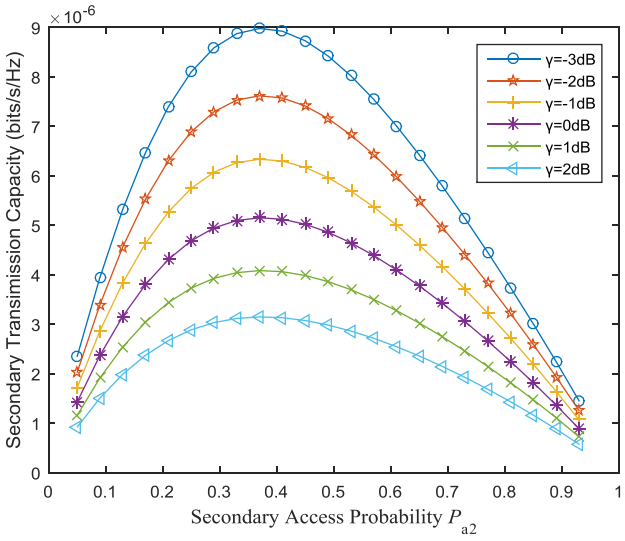

FIGURE 7. Secondary capacity under different SIR threshold with $D = 29$ and $\rho_2 = 1$.

SIR thresholds means more complicated hardware realization. Similarly, the transmission capacities vary apparently for different SIR thresholds with respect to access probabilities approximated in the range from 0.2 to 0.7. Again, we observe that the maximum capacity will be obtained when $P_{a2} \approx 0.4$ for different SIR thresholds.

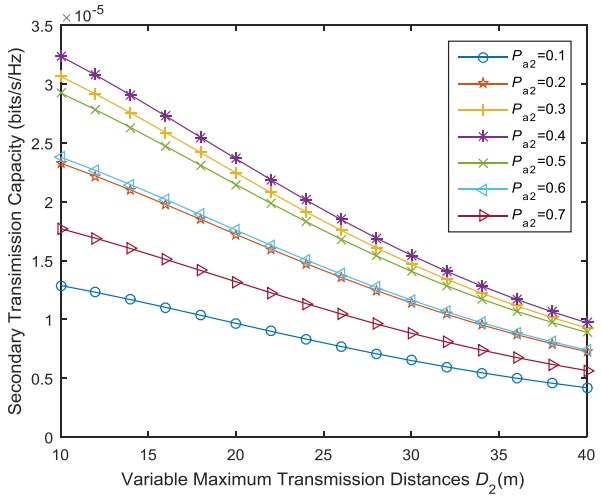

FIGURE 8. Secondary transmission capacity under different access probability with variable maximum distances D2 between source and destination.

Fig. 8 demonstrates the change of transmission capacity of the secondary network with variable maximum distances D_2 between source and destination with a fixed minimum distance $D_1 = 5$m. We can see that the capacity decreases with the maximum distance because the larger maximum distance will lead to longer average distance and greater attenuation. In addition, Fig. 8 indicates that there exists a maximum capacity when $P_{a2} = 0.4$, and each curve for P_{a2} close to 0.4 (e.g. $P_{a2} = 0.3$ and 0.5) is close to each other. Further, when the P_{a2}s are farther from 0.4 (e.g. $P_{a2} = 0.1$ and 0.7), the capacity curves become smaller and more gradual which is similar to the results obtained in Fig.4.

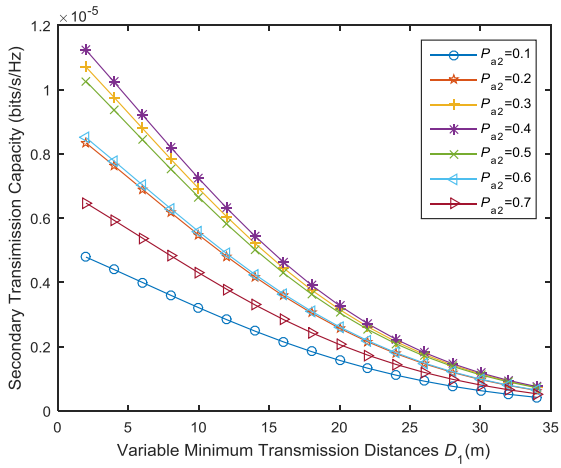

FIGURE 9. Secondary transmission capacity under different access probability with variable minimum distances D1 between source and destination.

Fig. 9 illustrates the change of transmission capacity of the secondary network with variable minimum distances with a fixed maximum distance $D_2 = 40$m. We can see small minimum distance brings high capacity which also changes sharply with P_{a2}. Similar to Fig.8, we can see that the maximum transmission capacity will be obtained when $P_{a2} = 0.4$ and each capacity is close to each other when P_{a2} is around 0.4 (e.g. $P_{a2} = 0.3$ and 0.5). Besides, when the P_{a2}s are farther from 0.4 (e.g. $P_{a2} = 0.1$ and 0.7), the capacity curves become smaller and more gradual. In addition, when the D_1 is larger than a given value, see $D_1 > 25$m, each capacity curve becomes small and approaches each other.

Fig. 10 depicts that the transmission capacity changes with the guard zone radius under different PTs' density λ_1. From Fig. 10, we can observe that the secondary transmission

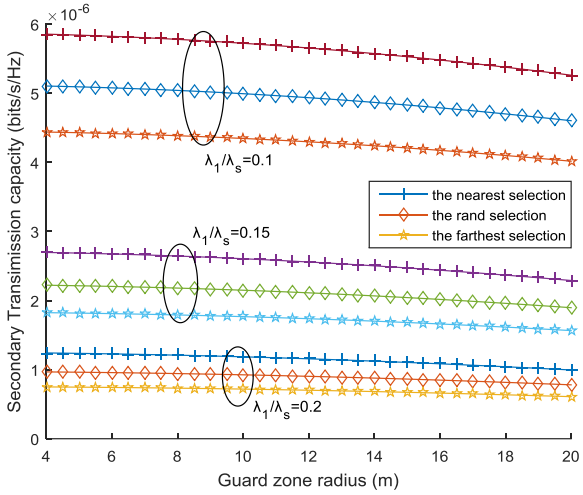

FIGURE 10. Secondary transmission capacity vs the guard zone radius as well as the density of λ_1.

capacity decreases slowly with increasing the guard zone radius because the larger PRs' radius means less transmission opportunity for secondary nodes. In addition, it is also shown that the secondary transmission capacity decreases faster with the increase of the density of primary transmitters. The reason is that more primary transmitters result in more severely interference to the secondary nodes.

V. CONCLUSIONS

In this paper, we investigate the transmission capacities of dual-hop underlay EH-CRSNs where both source and relay nodes are equipped with battery and operate in HSU model. First, we analyze the battery state when the transmission energy level threshold is set to be an arbitrary integer value with M/M/1/c model. Then, we derive the average distance and access probabilities for three kinds of relay selection schemes. Besides, based on stochastic geometry, the transmission capacity with harvesting battery relays is derived in closed-form expressions. Furthermore, we analyze the transmission capacity under variable source-destination distance following uniform distribution for three kinds of relay selection schemes. Next, simulation results demonstrate that the capacity is deeply influenced by some key parameters, such as source-destination distance, secondary access probability, battery capacity and transmission energy level threshold. Finally, by analyzing the simulations results of the underlay relay-assisted EH-CRSNs, we conclude that: (1) moderate secondary access probability value of approximate 0.35 can provide almost maximum transmission capacity; (2) using moderate instead of infinite battery capacity can obtain enough transmission capacity; and (3) compared with the nearest and the farthest relay selection, random relay selection scheme can provide a more feasible and reasonable transmission solution due to its simple implementation. As possible extensions, relay selection and resource allocation optimization in multi-hop EH-CRSNs will be investigated in future.

.

APPENDIX A

PROOF OF PROPOSITION 1

The cumulative distribution function (CDF) of X_n is:

$$\begin{aligned} F_{X_n|\Gamma\neq\emptyset}(x) &= 1 - P[X_n > x|\Gamma \neq \emptyset] \\ &= 1 - \frac{P[X_n > x, \Gamma \neq \emptyset]}{P[\Gamma \neq \emptyset]} \\ &= 1 - \frac{P[X_n > x] - P[X_n > x, \Gamma = \emptyset]}{P[\Gamma \neq \emptyset]} \\ &= 1 - \frac{\exp(-\frac{\theta\lambda_{an1}x^2}{2}) - \exp(-\frac{\theta\lambda_{an1}D^2}{2})}{1 - \exp(-\frac{\theta\lambda_{an1}D^2}{2})} \\ &= \frac{1 - \exp(-\frac{\theta\lambda_{an1}}{2}x^2)}{1 - \exp(-\frac{\theta\lambda_{an1}}{2}D^2)} \end{aligned}$$

where $\Gamma \neq \emptyset$ denotes that there exits at least one relay within the relaying region. Thus the probability density function (PDF) of X_n can be derived as

$$f_{X_n}(x) = \frac{\theta\lambda_{an1}x\exp(-\frac{\theta\lambda_{an1}}{2}x^2)}{1 - \exp(-\frac{\theta\lambda_{an1}}{2}D^2)}$$

Then the mean distance expression (9) can be obtained.

APPENDIX B

PROOF OF PROPOSITION 2

Applying the similar method illustrated in Appendix A, the CDF of X_f is

$$\begin{aligned} F_{X_f|\Gamma\neq\emptyset}(x) &= \frac{\Pr[X_f \leq x] - \Pr[X_f \leq x, \Gamma = \emptyset]}{\Pr[\Gamma \neq \emptyset]} \\ &= \frac{\exp(-\frac{\theta\lambda_{af1}(D^2-x^2)}{2}) - \exp(-\frac{\theta\lambda_{af1}D^2}{2})}{1 - \exp(-\frac{\theta\lambda_{af1}D^2}{2})} \\ &= \frac{\exp(\frac{\theta\lambda_{af1}x^2}{2}) - 1}{\exp(\frac{\theta\lambda_{af1}D^2}{2}) - 1} \end{aligned}$$

The PDF of X_f can be derived as

$$f_{X_n}(x) = \frac{\theta\lambda_{af1}x\exp(\frac{\theta\lambda_{af1}}{2}x^2)}{\exp(\frac{\theta\lambda_{af1}}{2}D^2) - 1}$$

Then the mean distance expression (12) can be obtained.

REFERENCES

[1] J. Ren, J. Hu, D. Zhang, H. Guo, Y. Zhang, and X. Shen, "RF energy harvesting and transfer in cognitive radio sensor networks: Opportunities and challenges," *IEEE Commun. Mag.*, vol. 56, no. 1, pp. 104–110, Jan. 2018.

[2] S. Aslam, W. Ejaz, and M. Ibnkahla, "Energy and spectral efficient cognitive radio sensor networks for Internet of Things," *IEEE Internet Things J.*, vol. 5, no. 4, pp. 3220–3233, Aug. 2018.

[3] M.-L. Ku, W. Li, Y. Chen, and K. J. R. Liu, "Advances in energy harvesting communications: Past, present, and future challenges," *IEEE Commun. Surveys Tuts.*, vol. 18, no. 2, pp. 1384–1412, 2nd. Quart., 2016.

[4] X. Zhang, Y. Zhang, Z. Yan, J. Xing, and W. Wang, "Performance analysis of cognitive relay networks over Nakagami-*m* fading channels," *IEEE J. Sel. Areas Commun.*, vol. 33, no. 5, pp. 865–877, May 2015.

[5] Z. Wang, Z. Chen, B. Xia, L. Luo, and J. Zhou, "Cognitive relay networks with energy harvesting and information transfer: Design, analysis, and optimization," *IEEE Trans. Wireless Commun.*, vol. 15, no. 4, pp. 2562–2576, Apr. 2016.

[6] X. Liu, F. Li, and Z. Na, "Optimal resource allocation in simultaneous cooperative spectrum sensing and energy harvesting for multichannel cognitive radio," *IEEE Access*, vol. 5, pp. 3801–3812, 2017.

[7] W. Lu, Y. Gong, X. Liu, J. Wu, and H. Peng, "Collaborative energy and information transfer in green wireless sensor networks for smart cities," *IEEE Trans. Ind. Informat.*, vol. 14, no. 4, pp. 1585–1593, Apr. 2018.

[8] I. Krikidis, G. Zheng, and B. Ottersten, "Harvest-use cooperative networks with half/full-duplex relaying," in *Proc. IEEE WCNC*, Shanghai, China, Apr. 2013, pp. 4256–4260.

[9] S. Lee, R. Zhang, and K. Huang, "Opportunistic wireless energy harvesting in cognitive radio networks," *IEEE Trans. Wireless Commun.*, vol. 12, no. 9, pp. 4788–4799, Sep. 2013.

[10] X. Chen, X. Meng, X. Song, Y. Geng, and C. Shan, "Coverage probability in cognitive radio networks powered by renewable energy with primary transmitter assisted protocol," *Inf. Sci.*, vols. 400–401, pp. 14–29, Aug. 2017.

[11] S. Gautam, X. V. Thang, S. Chatzinotas, and B. Ottersten, "Cache-aided simultaneous wireless information and power transfer (SWIPT) with relay selection," *IEEE J. Sel. Areas Commun.*, vol. 37, no. 1, pp. 187–201, Jan. 2019.

[12] T. A. Khan, P. V. Orlik, K. J. kim, R. W. Heath, Jr., and K. Sawa, "A stochastic geometry analysis of large-scale cooperative wireless networks powered by energy harvesting," *IEEE Trans. Commun.*, vol. 65, no. 8, pp. 3343–3358, Aug. 2017.

[13] J. Jeon and A. Ephremides, "On the stability of random multiple access with stochastic energy harvesting," *IEEE J. Sel. Areas Commun.*, vol. 33, no. 3, pp. 571–584, Mar. 2015.
[14] R. Vaze, "Transmission capacity of wireless ad hoc networks with energy harvesting nodes," in *Proc. IEEE Global Conf. Signal Inf. Process.*, Austin, TX, USA, Dec. 2013, pp. 353–358.
[15] Y. Huang, F. Al-Qahtani, C. Zhong, Q. Wu, J. Wang, and H. Alnuweiri, "Performance analysis of multiuser multiple antenna relaying networks with co-channel interference and feedback delay," *IEEE Trans. Commun.*, vol. 62, no. 1, pp. 59–73, Jan. 2014.
[16] J. A. Hussein, S. S. Ikki, S. Boussakta, and C. C. Tsimenidis, "Performance analysis of opportunistic scheduling in dual-hop multiuser underlay cognitive network in the presence of cochannel interference," *IEEE Trans. Veh. Technol.*, vol. 65, no. 10, pp. 8163–8176, Oct. 2016.
[17] Z. Yang, Z. Ding, P. Fan, and G. K. Karagiannidis, "Outage performance of cognitive relay networks with wireless information and power transfer," *IEEE Trans. Veh. Technol.*, vol. 65, no. 5, pp. 3828–3833, May 2016.
[18] S. A. R. Zaidi, M. Ghogho, A. Swami, and D. C. McLernon, "Achievable spatial throughput in multi-antenna cognitive underlay networks with multi-hop relaying," *IEEE J. Sel. Areas Commun.*, vol. 31, no. 8, pp. 1543–1558, Aug. 2013.
[19] Y. Liu, S. A. Mousavifar, Y. Deng, C. Leung, and M. Elkashlan, "Wireless energy harvesting in a cognitive relay network," *IEEE Trans. Wireless Commun.*, vol. 15, no. 4, pp. 2498–2508, Apr. 2016.
[20] Z. Yan, S. Chen, X. Zhang, and H. L. Liu, "Outage performance analysis of wireless energy harvesting relay-assisted random underlay cognitive networks," *IEEE Internet Things J.*, vol. 5, no. 4, pp. 2691–2699, Aug. 2018.
[21] A. M. Siddiqui, L. Musavian, S. Aïssa, and Q. Ni, "Performance analysis of relaying systems with fixed and energy harvesting batteries," *IEEE Trans. Commun.*, vol. 66, no. 4, pp. 1386–1398, Apr. 2018.
[22] I. Krikidis, "Relay selection in wireless powered cooperative networks with energy storage," *IEEE J. Sel. Area Commun.*, vol. 33, no. 12, pp. 2596–2610, Dec. 2015.
[23] G. Noh, S. Lim, and D. Hong, "Exact capacity analysis of spectrum sharing systems: Average received-power constraint," *IEEE Commun. Lett.*, vol. 17, no. 5, pp. 884–887, May 2013.
[24] Y. Yang, Y. Zhang, L. Dai, J. Li, S. Mumtaz, and J. Rodriguez, "Transmission capacity analysis of relay-assisted device-to-device overlay/underlay communication," *IEEE Trans. Ind. Informat.*, vol. 13, no. 1, pp. 380–389, Feb. 2017.
[25] C. Xu, M. Zheng, W. Liang, H. Yu, and Y. Liang, "End-to-end throughput maximization for underlay multi-hop cognitive radio networks with RF energy harvesting," *IEEE Trans. Wireless Commun.*, vol. 16, no. 6, pp. 3561–3572, Jun. 2017.
[26] M. Haenggi, *Stochastic Geometry for Wireless Networks*. Cambridge, U.K.:Cambridge Univ. Press, 2013.
[27] Y. Gu, H. Chen, Y. Li, Y. C. Liang, and B. Vucetic, "Distributed multi-relay selection in accumulate-then-forward energy harvesting relay networks," *IEEE Trans. Green Commun. Netw.*, vol. 2, no. 1, pp. 74–86, Mar. 2018.
[28] W. J. Stewart, *Probability, Markov Chains, Queues, and Simulation: The Mathematical Basis of Performance Modeling*. Princeton, NJ, USA: Princeton Univ. Press, 2009.
[29] I. S. Gradshteyn and I. M. Ryzhik, *Table of Integrals, Series, and Products*, 6th ed. New York, NY, USA: Academic, 2000.
[30] X. Wu and Z. Gu, "A joint time synchronization and localization method without known clock parameters," *Pervasive Mobile Comput.*, vol. 37, pp. 154–170, Jun. 2017.
[31] W. Meng, D. Zhang, Y. Wang, and C. Li, "An extended centroid localization algorithm based on error correction in WSN," in *Proc. IEEE Global Commun. Conf.*, Austin, TX, USA, Dec. 2014, pp. 442–447.

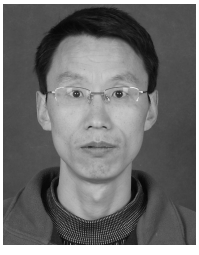

HONG JIANG received the Ph.D. degree from the School of Communication and Information Engineering, University of Electronic Science and Technology of China, China, in 2004. He is currently a Full Professor with the Southwest University of Science and Technology, China. His current research interests include the cross-layer QoS support in ad hoc networks, energy harvesting, the Internet of Things, optimization, and intelligent learning for resource management in cognitive radio networks.

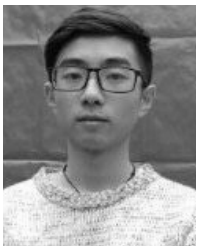

HAO YANG received the B.S. degree from the Department of Information Engineering, Southwest University of Science and Technology (SWUST), in 2017, where he is currently pursuing the master's degree. His research interests include wireless sensor networks, optimization, and analysis.

YING LUO received the B.S. and M.S. degrees from the Department of Information Engineering, Southwest University of Science and Technology (SWUST), in 2012 and 2015, respectively, and the Ph.D. degree from the Department of Electronic Engineering and Information Science (EEIS), University of Science and Technology of China (USTC), in 2018. She is currently a Teacher with the Department of Information Engineering, SWUST. Her research interest includes next-generation networks.

QIUYUN ZHANG received the B.S. and M.S. degrees from the Department of Information Engineering, Southwest University of Science and Technology (SWUST), in 2011 and 2014, respectively, where he is currently pursuing the Ph.D. degree. His research interests include the optimization and analysis of wireless networks.

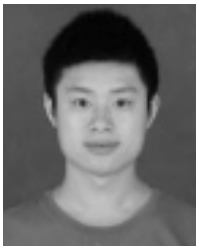

MIN ZENG received the B.S. and M.S. degrees from the Department of Information Engineering, Southwest University of Science and Technology (SWUST), in 2012 and 2015, respectively, where he is currently pursuing the Ph.D. degree. His research interests include the analysis of green communications and the IoT networks.